Available on CMS information server

**CMS NOTE 2000/024**

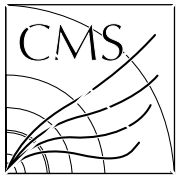


**The Compact Muon Solenoid Experiment**

**CMS Note**

Mailing address: CMS CERN, CH-1211 GENEVA 23, Switzerland

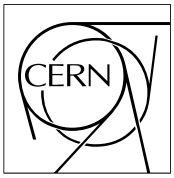


# First evaluation of neutron induced Single Event Effects on the CMS barrel muon electronics

*S. Agosteo[1], L. Castellani[2], G. D'Angelo[1], A. Favalli[1], I. Lippi[2], R. Martinelli[2] and P. Zotto[3]*

1) Dip. di Ingegneria Nucleare (CESNEF) del Politecnico di Milano, Italy
2) Dip. di Fisica dell'Università and sez. INFN di Padova, Italy
3) Dip. di Fisica del Politecnico di Milano and sez. INFN di Padova, Italy

**Abstract**

Neutron irradiation tests of the currently available electronics for the CMS barrel muon detector were performed using thermal and fast neutrons at E < 11MeV. The Single Event Upset rate on the Static RAM was measured, while upper limits are derived for devices having experienced no failure. The results are used to guess the upper limits on the mean time between failures in the whole barrel muon detector.

## 1. Introduction

The LHC detectors will be working inside the highest radiation ever experienced in high energy physics. Several studies were done in order to check the radiation tolerance of the detector itself and investigations were done in order to assess the tolerance of electronics.

The barrel muon chambers are a particular case within the general scenario. The radiation dose absorbed after ten years of operation at LHC is negligible (less than 0.2Gy). The expected neutron fluence is not high enough to generate a relevant bulk damage (less than $2.5 \times 10^{10}$ n/cm$^2$), nevertheless detector electronics could still be disturbed or even damaged because of Single Event Effects. Besides it will not be accessible, since most of it is located within the cavern, lodged on the chambers.

We expect therefore that most of the reliability of these electronics will be associated to the probability of occurrence of rare Single Event Effects (SEE) induced by the interaction with the silicon chips of the ionizing particles.

## 2. Neutron background expectations

Muon chambers are shielded by the iron yoke against the effects of charged low energy particles, and the background particle flux will be dominated by neutrons thermalizing within the cavern. Neutrons are produced all around inside the cavern by beam halo interactions with magnets on the LHC beam line and the detector itself.

Extensive simulation studies [1] were done to estimate the rate of background particles at all positions inside CMS. The results of the simulation are shown in Figure 1, where we immediately see that the flux is quite low. In particular the energy spectra of neutrons were determined. Although the Montecarlo calculations for low energy neutrons are usually affected by large errors, we have a determination of the expected neutron rate. We also see that the neutron background is linearly decreasing with energy and is naturally ending around 100 MeV in the outermost station and at few hundred MeV in the innermost one, that is suffering from high energy neutrons flooding through the CMS calorimeters and coil.

## 3. Single Event Effects phenomenology

The Single Event Effects are associated to individual ionizing particles and their occurrence is given as a cross section.

The most likely common effect is called Single Event Upset (SEU) and affects all kinds of memory devices (SRAM, DRAM and FLASH memories, microprocessors and DSP, FPGA and logic programmable state machines, etc.). It is detected as a modification of the memory state and is usually recoverable by data rewriting. Memory upset is caused by the deposition, inside a device sensitive node, of a charge higher than a given threshold. This charge value is dependent on both technology and device layout [2]. Even system architecture plays a relevant role in SEU sensitivity: a careful system design helps in reducing the probability of device damaging as a by-product of a single event [3]. Critical data can be protected either using less sensitive technologies or implementing redundant logic. Occasionally the energy deposition associated to the interacting particle can be the cause of a latch-up (SEL) or a gate rupture (SEGR) or even a device burnout (SEBO) [4]: these effects could be destructive and generally cannot be recovered. Both SEL and SEBO effects can be reduced by system architecture design. As a matter of fact, while the permanent damage associated to SEL can be eliminated using power supply and input-output overcurrent protection circuitry, the power device burnout probability can be reduced to a safety level limiting the operating voltage to a fraction of the breakdown value.

SEE, usually considered when designing aerospatial instrumentation, are a major concern for LHC detectors where the ionizing particle background level is high enough to foresee an important number of SEE. All the measurements done

until now confirm that the SEU probability is depending both on the technology used for integrated circuits production and on the processing chain actually used in the factory. The associated technological parameters are usually not well controlled since two orders of magnitude in the quoted results are a typical variation. Simulations [5] have shown that standard manufacturing process tolerances (usually in the range of a factor 2) can result in variations in the single event rates of a factor 60. Furthermore very recent tests [5] proved that also thermal neutrons are causing SEU. The responsible mechanism could be neutron capture from the $^{10}B$ isotope (19.9% of natural boron), normally present in semiconductor technologies as a result of doping and in the glass passivation layer, followed by nucleus de-excitation with $\alpha$-particle emission through the reaction $^{10}B(n,\alpha)^{7}Li$. Both the lithium nucleus and the $\alpha$-particle release locally enough energy to cause the memory cell change of state [5,6].

Fast neutrons interact with $^{28}Si$ atoms producing relevant recoil energy already at neutron energy around 0.1 MeV. Only neutrons with an incident energy higher than 3 MeV can contribute to the measured cross section: the relevant reactions are in fact $^{28}Si(n,p)^{28}Al$ with a 4 MeV threshold and $^{28}Si(n,\alpha)^{25}Mg$ with a 2.7 MeV threshold [6]. Furthermore recoil maximum energy saturates around 2.5 MeV/(mg/cm$^2$) already for neutrons of 20MeV [7]. Published results claim that SEU cross section has an energy threshold and is slowly increasing with energy up to a saturation value correspondent to

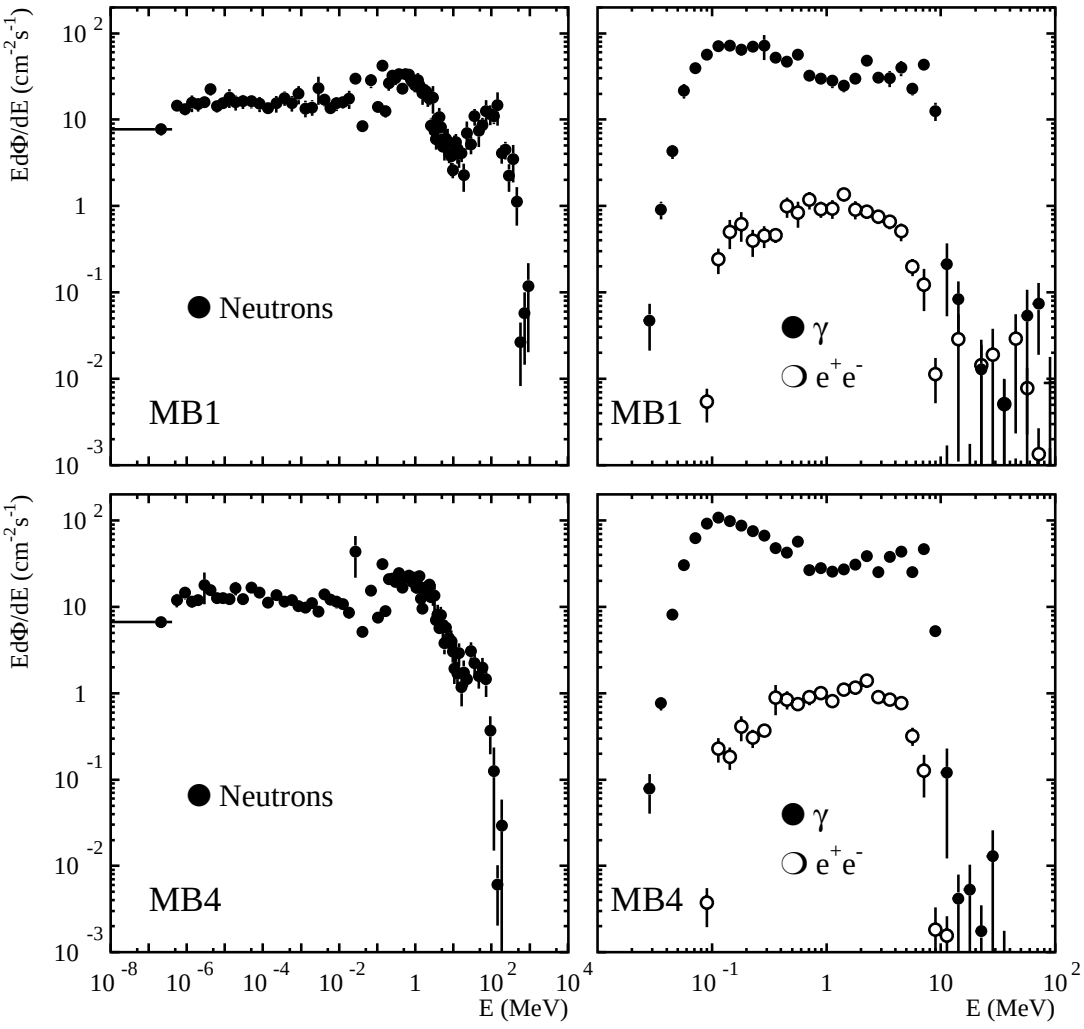


Figure 1 – Expected neutral particle fluence through the innermost (MB1) and the outermost (MB4) muon barrel stations.

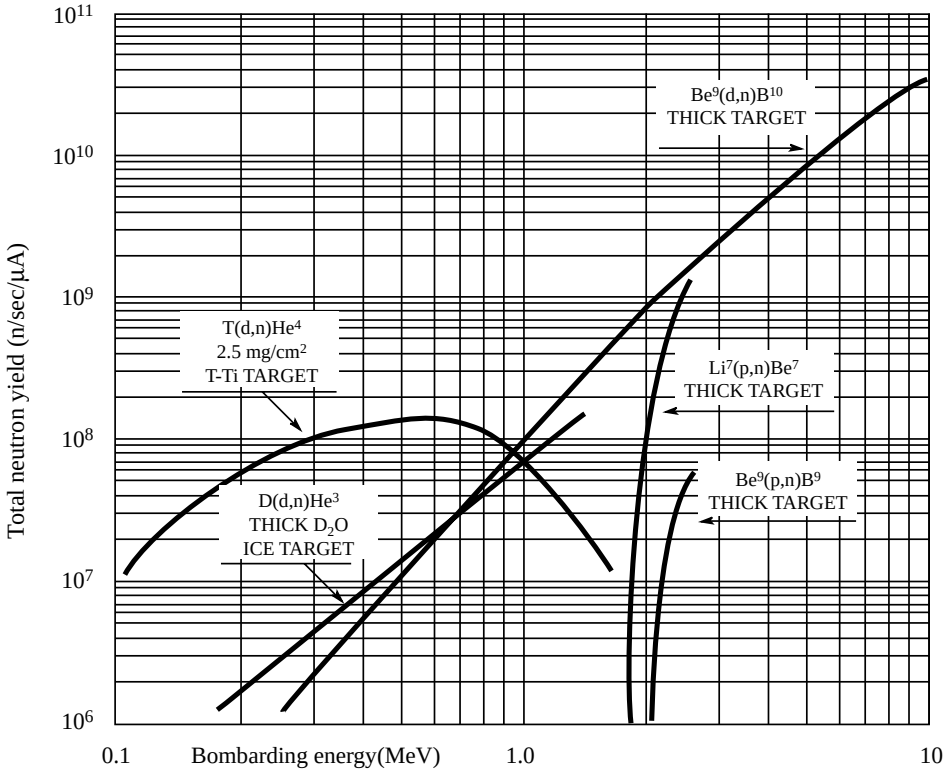


Figure 2 – Total neutron yield in some typical nuclear reactions.

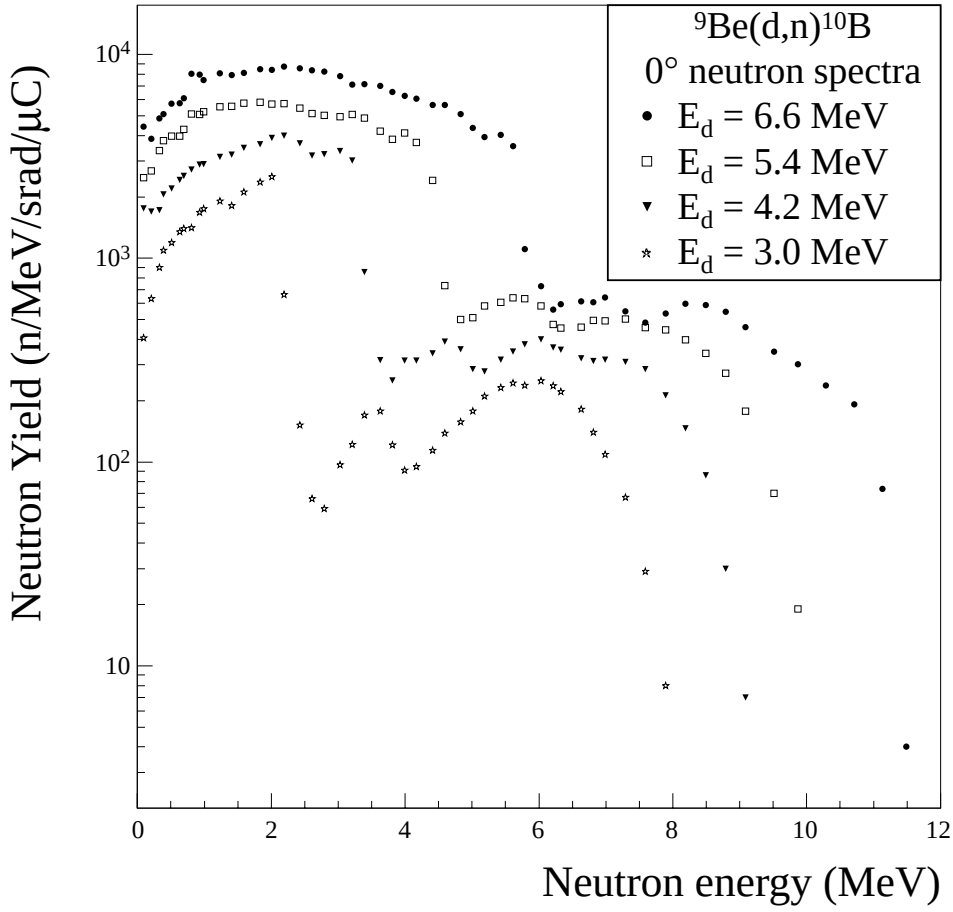


Figure 3 – The 0° neutron production spectra in the $^{9}Be(d,n)^{10}B$ reaction.

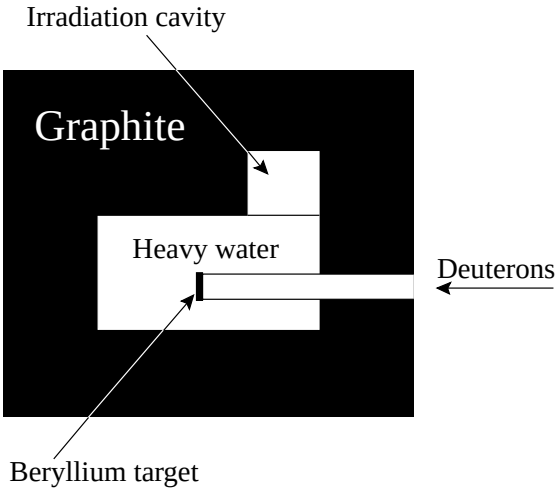


Figure 4 – Sketch of the neutron moderator used for the test with thermal neutrons.

100 MeV neutrons [8].

Since, as many published works show, neutron and proton SEU cross-sections are very similar for energies higher than 20 MeV [6], it might be stated that testing with high energy protons could be a reasonable procedure to qualify components to be operated with consistent neutron fluxes [9].

However comparison of measurements of the proton induced SEU cross-section to the neutron induced SEU cross section show that they are somewhat different: the first one is steeper with incident energy than the second one and it seems to saturate at a higher energy. Assuming that the same reaction products are responsible for the SEU, this fact was explained considering Coulomb barrier effects in proton interactions [6,8,10]. Besides different nuclear properties and cross section for secondary particles production by neutrons and protons must be taken into account. Furthermore the ionizing dose deposition associated to proton irradiations were considered responsible for observed “data imprinting” effects (i.e. the devices cannot be reprogrammed and some random data is fixed in the memory location), frequently leading to underestimated values of the SEU cross-section [11]. The lack of truly mono-energetic neutron sources for irradiation tests has not allowed researchers to study experimentally the similarity between proton and neutron cross-sections for SEE production. In this scenario, the whole existing literature agrees that, if the neutron background is going to be a problem, the existing data cannot be used directly to estimate SEU probability, unless you can tolerate large safety margins. It is therefore recommended to get oneself own measurements done .

## 4. Measurements setup

CMS barrel muon detector electronics will deal with a wide spectrum of neutron energies. Our first irradiation tests aim to evaluate effects due to the fast neutrons below 10 MeV or the thermal portion of the neutron spectrum.

Low energy neutrons are copiously produced in the nuclear laboratories by scattering of proton or deuteron nuclei accelerators on low atomic mass nuclei targets.

At the nuclear INFN laboratory of Legnaro a deuteron beam accelerated at 7 MeV by a Van de Graaff accelerator interacts with a thick beryllium target producing neutrons through the reaction $^{9}Be(d,n)^{10}B$. The neutron rate, shown in Figure 2, is high enough to allow an easy integration often LHC years in a reasonably short time. The emitted neutron spectrum [12] is shown in Figure 3 for several incident deuteron energies. The neutron spectra high-end is limited to about $E_n$ = 11MeV.

Thermal neutrons were generated using the same reaction. The moderator [13] is sketched in Figure 4. The Beryllium target is enclosed in an heavy water tank surrounded by very thick graphite walls. The fast neutrons produced in the d-Be scattering are therefore moderated by the heavy water and reflected from the graphite, thermalizing and remaining inside the graphite. The irradiation cavity is situated on top of the heavy water tank in backward position with respect to the beryllium target in order to minimize the residual fast neutron content. The neutron spectra calculated using the MCNP Montecarlo code inside the irradiation cavity is shown in Figure 5, while Figure 6 shows the measurements done to verify the uni-

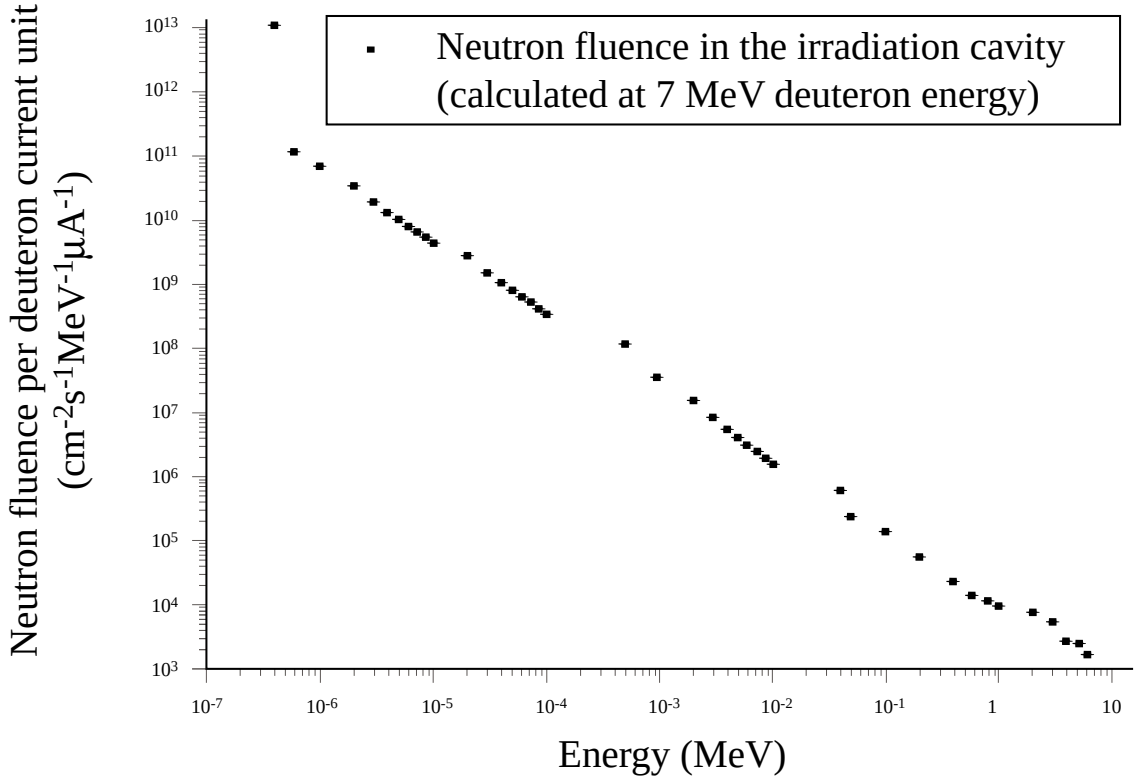


Figure 5 – Neutron fluence in the irradiation cavity. The thermal neutrons are falling in the first bin of the plot. Thermal neutrons (E < 0.4 eV) fluence is one order of magnitude higher than epithermal neutrons (0.4eV < E < 10keV) fluence and two orders of magnitude higher than fast neutrons (E > 10keV).

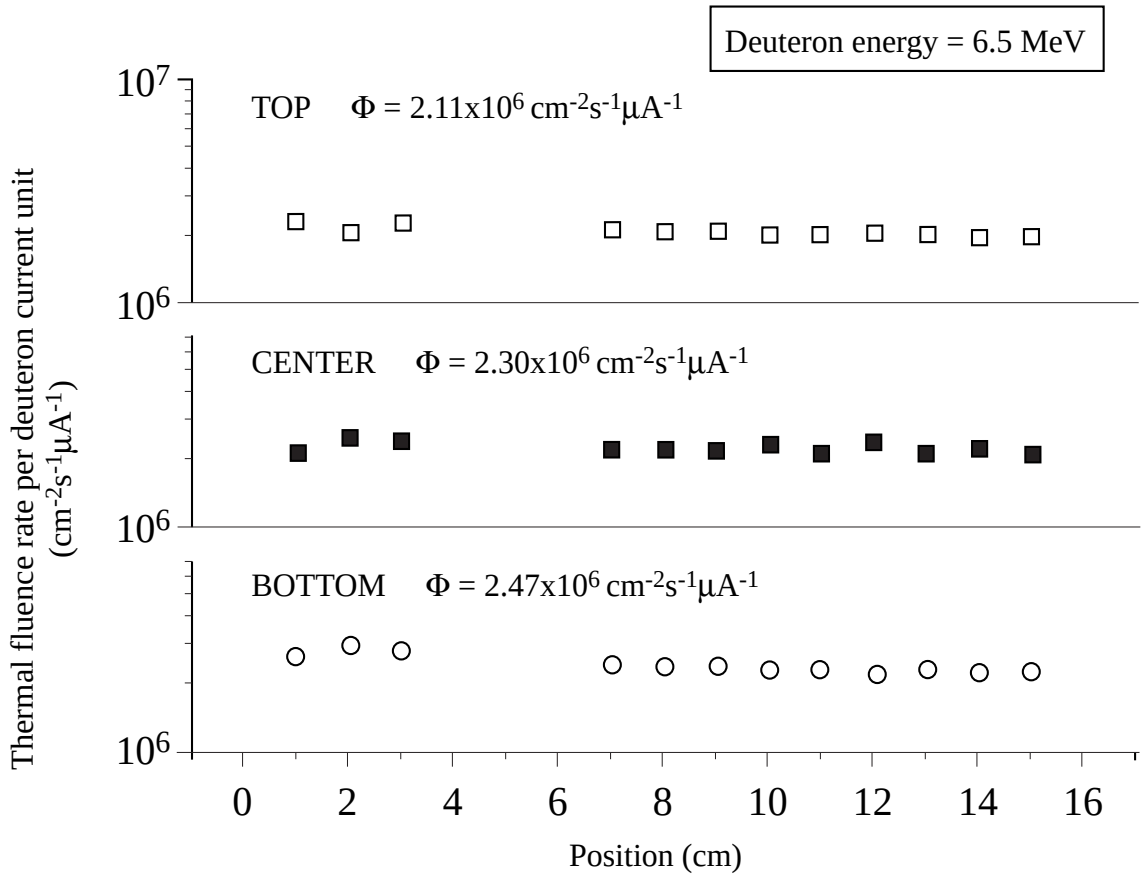


Figure 6 – Measurement of the uniformity of the neutron flux inside the irradiation cavity.

| Board | Component | Productor / Type / Year |
|---|---|---|
| Slow control | LD Regulator | MICREL / 29501-3.3BU / 1997 |
| | µP | MOTOROLA / MC68HC16 / 1994 |
| | FLASH | ATMEL / AT29C101A-12PC / 1996 |
| | SRAM#1 | SONY / CXK581000AM-70LL / 1993 |
| | SRAM#2 | SONY / CXK581000AM-70LL / 1993 |
| | EPROM | ATMEL / AT27C512R-15JC / 1995 |
| | Optical transceiver | HONEYWELL/ HFM2600-1 / 1998 |
| Trigger | ASIC TSS | ES2 0.7 µm / TOP5 ceramic package / 1997 |
| | ASIC BTI | ATMEL 0.5 µm / LTCC substrate & in dies /1997 |
| Front-end | ASIC MAD | AMS 0.8 µm / BCMOS / 1997 |

Table 1 – List of tested components with relevant characteristics of each device.

formity inside the cavity.

The devices ready to be tested in 1999 were the first prototype of the slow control board, the readout front-end board, the front-end trigger device and a prototype trigger server board.

The list of relevant integrated circuits is shown in Table 1.

Device registers were initialized to a standard pattern, verified by the readout system with a two seconds cycle. Every time an alteration of the memory state was detected, the time, the integrated current on the target, the address and the datum were stored on disk for data analysis.

## 5. SEU cross section with thermal neutrons

The boards were irradiated with thermal neutrons on four data taking periods. Since the neutron flux inside the graphite is modified by the inserted boards, we had to get the actual neutron flux measuring the activation of Indium and Cadmium-Indium ( to subtract non thermal contribution) targets placed just in front of the integrated circuits.

The only device experiencing SEU was SRAM#1. Figure 7 shows the plot of the

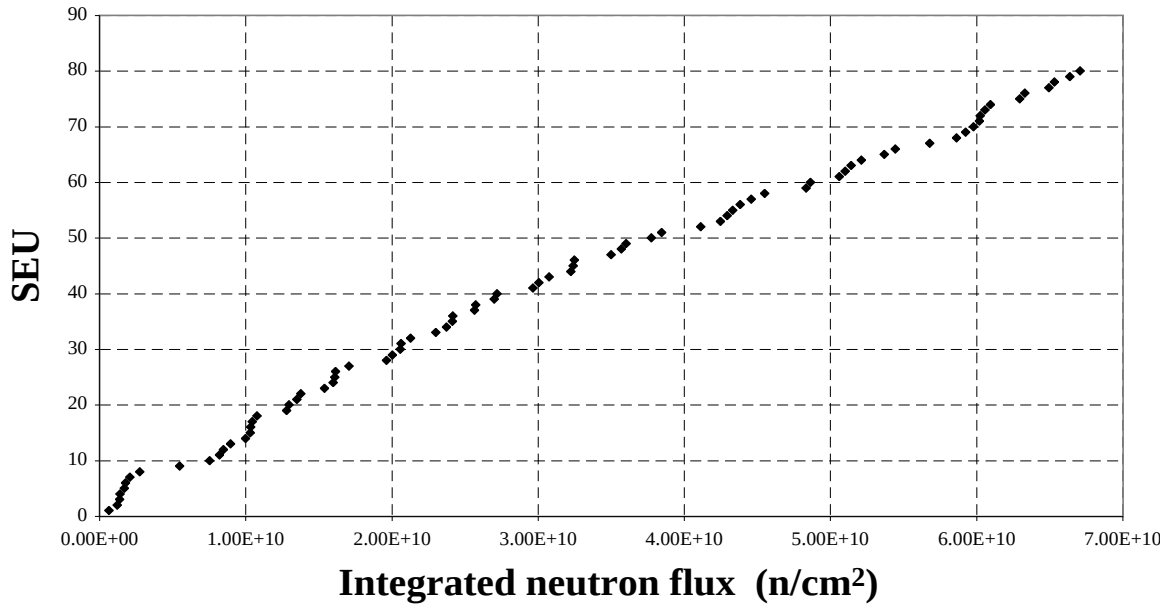


Figure 7 – SEU progressive number versus integrated neutron flux in the thermal neutron run. The line is the measured SEU cross section evaluation.

| Component | Total rate $n/cm^2$ | Device SEU cross section $cm^2$ | Mean time between failures in the full detector hh:mm |
|---|---|---|---|
| LD Regulator | $6.87x10^{10}$ | $< 1.38x10^{-10}$ | > 64:19 |
| µP | $6.87x10^{10}$ | $< 1.38x10^{-10}$ | > 385:56 |
| FLASH | $6.87x10^{10}$ | $< 1.38x10^{-10}$ | > 385:56 |
| SRAM#1 | $6.87x10^{10}$ | $(1.13\pm0.2)x10^{-9}$ | 23:34 |
| SRAM#2 | $6.87x10^{10}$ | $< 1.38x10^{-10}$ | > 192:58 |
| EPROM | $6.87x10^{10}$ | $< 1.38x10^{-10}$ | > 385:56 |
| Optical transceiver | $6.87x10^{10}$ | $< 1.38x10^{-10}$ | > 385:56 |
| ASIC TSS | $2.36x10^{10}$ | $< 2.68x10^{-10}$ | > 33:09 |
| BTI | $5.69x10^{10}$ | $< 1.75x10^{-10}$ | > 1:35 |
| MAD | $9.10x10^{9}$ | See dedicated section | |

Table 2 –SEU cross section and estimates of mean time between failures in the full barrel muon detector due to thermal neutrons interactions. The limits are 90% C.L.

SEU numbers versus the integrated neutron dose for all the test periods. The slope of the average line fitted in this plot is a measurement of the SEU cross section of the device. We can only quote a 90% confidence level upper limit of the SEU cross section for all the other tested integrated circuits. Indeed we had a Low Drop Regulator fault detected by the system after integrating $7x10^9$ $n/cm^2$, but we feel safer quoting only the upper limit rather than the quite low SEU cross section. Results of the thermal neutron runs are summarized in Table 2. The error in SRAM#1 SEU cross section evaluation is essentially systematic: we quote the spread in the calculation between the four different data taking periods. The Mean Time Between Failures is computed for the whole barrel muon detector, considering the number of pieces of each chip used in the electronics layout. We considered 50000 BTI chips and about 1000 pieces of the other devices.

## 6. SEU cross section with fast neutrons

As we already stressed there is some evidence that the SEU cross section for fast neutron will be dependent on the neutron energy. As evidenced by the momentum spectra of Figure 3, the neutrons produced by the $^9Be(d,n)^{10}B$ reaction are not monochromatic. The measurements with the thick Beryllium targets are nonetheless useful to give an indication of the existence of fast neutrons induced SEU.

### 6.1 Overview of the observed effects

In order to reduce the data taking period to a reasonable amount of time we had to place the boards quite close to the target (few centimeters), with the deuteron beam line being centred on each component to be tested for a short time. Under this conditions the neutron flux is far from being uniform through the devices. Besides, every time one of the integrated circuits is irradiated, the neutron flux on the others is not negligible. Therefore we had to estimate for each period, the amount of integrated neutron dose on each circuit applying neutron angular distributions and geometrical corrections.

We used the MCNP Montecarlo code to determine the neutrons flux expected through our devices with a careful description of the setup area in order to account for neutrons scattering on the walls, the floor and on the relevant devices inside the measurement area. The neutron flux angular distribution, as obtained by the Montecarlo, is shown in Figure 8. It is well fitted by a form $\Phi = b \cos^n\theta$ with $b = (1.29 \pm 1.71)$ X $10^7$ $n/cm^2$ and $n = 1.63\pm0.4$.

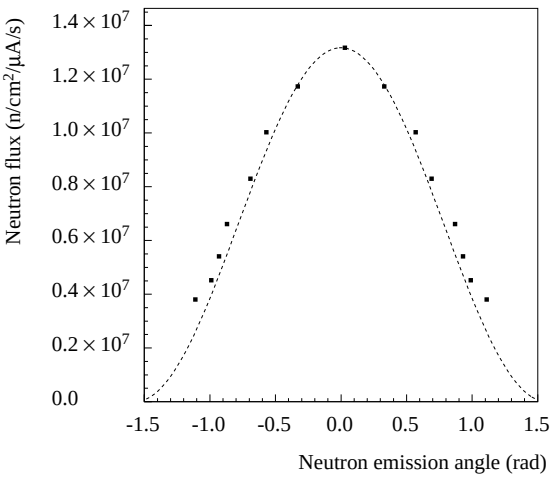


Figure 8 - Angular distribution of neutrons at 2 cm from the Beryllium target.

As expected after the thermal neutron test, we had a large number of SEU from SRAM#1. The SEU number at $E_d$ = 6.5MeV is shown as a function of time in Figure 9. The different slopes visible in the plot are an indication of how close was the SRAM to the beam line in each period. As we stated before we have to apply a geometrical correction factor to each data period in order to determine the amount of flux intercepted by the each device. These factors were calculated using the expected angular distribution. Applying the correction to SRAM#1 data, we obtained the plot of Figure 10, showing that our model of the neutron spatial distribution is satisfactory, since all periods exhibit the same slope.

The fact that the results are sitting on a line is an indication that there are no total dose effects, i.e. no saturation due to device degradation.

With fast neutrons we could observe also SEU on SRAM#2. Although this RAM is of the same type and production lot, we obtained a SEU cross section two orders of magnitude lower than SRAM#1 (4 SEU after $1.52 \times 10^{12}$ n/cm$^2$ against 135 SEU after $0.75 \times 10^{12}$ n/cm$^2$). Thus we experienced the effect reported in the existing literature of big variations for the same device.

We also had some cases of microprocessor faults: most of the cases are easily associated to corruption of the program inside the RAM and were solved by automatic program reload. But in at least one case we had a complete block of the system forcing to give an external hardware reset. As for the case of the LD Regulator fault we prefer to provide a SEU cross section upper limit.

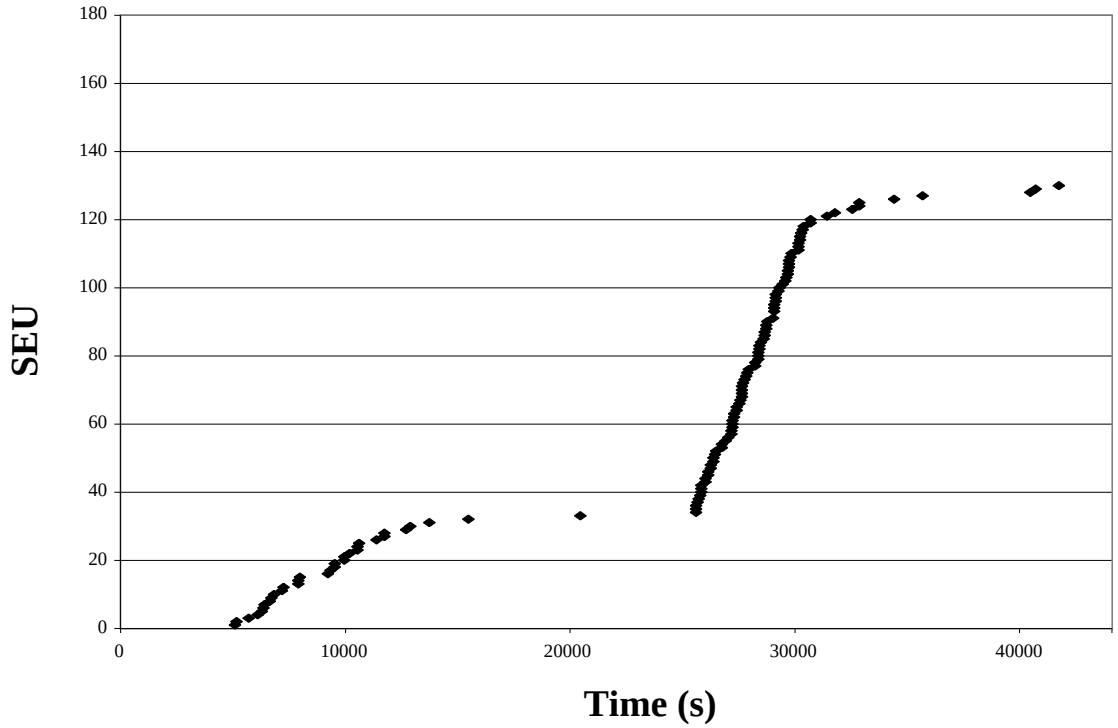


Figure 9 – SEU progressive number on SRAM#1 versus test time at $E_d$ = 6.5 MeV. The differences in slope and density is due to different incident positions of the deuteron beam.

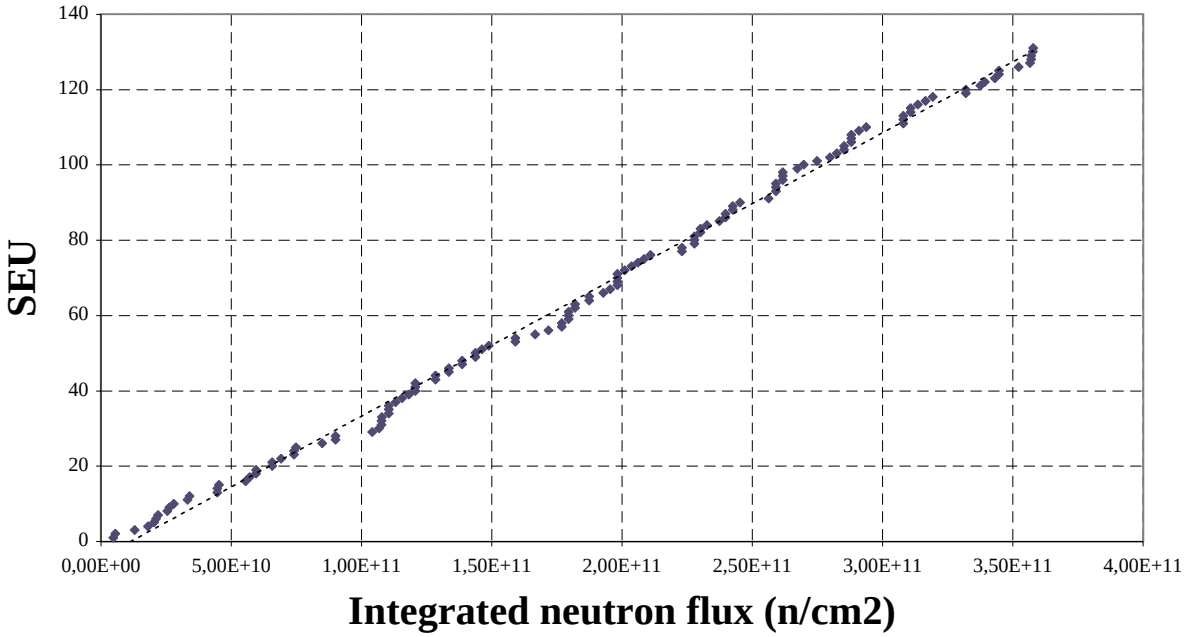


Figure 10 - SEU progressive number on SRAM#1 versus integrated neutron flux at $E_d$ = 6.5 MeV

Results are collected in Table 3: the quoted numbers presumes that neutrons of any energy have the same probability to cause a SEU, i.e. we did not allow neither any threshold nor any energy dependence in the SEU cross section. The error is the squared sum of statistical and systematical error. The systematical error is due to the uncertainty of the total neutron flux and is dominating our calculation.

Using the spectrum of Figure 3 and the Montecarlo results we can quote a cross section $\sigma_{SEU} = (7.03 \pm 0.2) \times 10^{-10}$ cm$^2$ on SRAM#1 if we consider that the upsets are due only to neutrons with energy $E_n > 3$MeV.

### 6.2 SEU uniformity verification

It is interesting to check if there are more sensitive positions inside the SRAM, or if the probability of a SEU happening inside the chip is equally distributed.

We verified that the address was not

| **Component** | **Total rate** n/cm$^2$ | **Device SEU cross section** cm$^2$ | **Mean time between failures in the full detector** hh:mm |
|---|---|---|---|
| LD Regulator | $9.69\times10^{11}$ | $< 9.79\times10^{-12}$ | > 907:42 |
| µP | $9.71\times10^{11}$ | $< 9.77\times10^{-12}$ | > 5457:34 |
| FLASH | $9.28\times10^{11}$ | $< 1.02\times10^{-11}$ | > 5214:56 |
| SRAM#1 | $5.74\times10^{11}$ | $(3.76\pm1.31)\times10^{-10}$ | 70:54 |
| SRAM#2 | $1.16\times10^{12}$ | $(2.29\pm1.55)\times10^{-12}$ | 14561:46 |
| EPROM | $8.46\times10^{11}$ | $< 1.12\times10^{-11}$ | > 4753:40 |
| Optical transceiver | $9.50\times10^{11}$ | $< 9.99\times10^{-12}$ | > 5336:52 |
| ASIC TSS | $1.44\times10^{12}$ | $< 6.61\times10^{-12}$ | > 2016:25 |
| BTI | $1.03\times10^{12}$ | $< 9.18\times10^{-12}$ | > 29:02 |
| MAD | $6.30\times10^{10}$ | see dedicated section | |

Table 3 –SEU cross section and estimates of mean time between failures in the full barrel muon detecto due to fast neutrons interactions. The limits are 90% C.L.

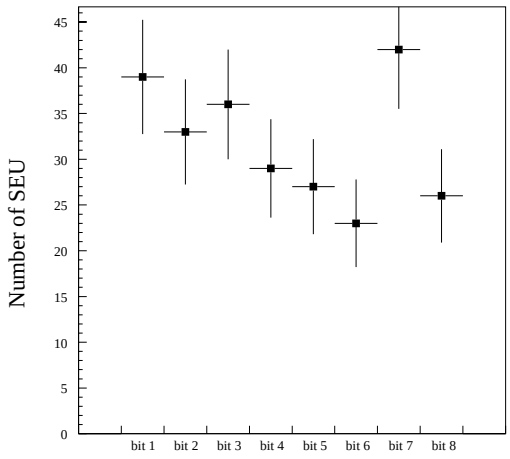


Figure 11 – Map of the bit flip occurred during the fast neutrons run

always the same and that also the bit of the data word changed was not repeating. The number of SEU on the fast neutron run is shown in Figure 11: within the statistics precision there is not any preferred bit flipping.

Another interesting check is the verification if the bit change from High → Low was more probable than the one from Low → High. Figure 12, taken from a thermal neutron run, supports the understanding of an homogeneity of the SEU cross section.

## 7. SEE on muon front-end integrated circuit

The readout front-end electronics is composed by a charge integrator and a variable threshold discriminator. Since the front-end circuit is a charge sensitive device, the SEE associated to it is the detection of energy deposition inside the integrated circuit simulating a pulse over threshold.

Two prototypes were tested both on thermal and fast neutrons. Since access to the boards was easier, in the fast neutron test we modified the threshold settings in order to verify that SEE cross section was depending on the actual threshold.

The result for thermal neutrons run is shown in Figure 13, while Figure 14 reports the SEE cross section in the threshold scan run for fast neutrons. Also in this case the quoted SEE cross section assumes that all neutrons in the spectrum have the same probability to induce a SEE. The systematic errors cannot be estimated, but the result is well below the input noise expected from interactions inside the gas volume. Hence, even in case of on order of magnitude error, we can state that we don't expect problems with noise induced from SEE on the front end readout electronics

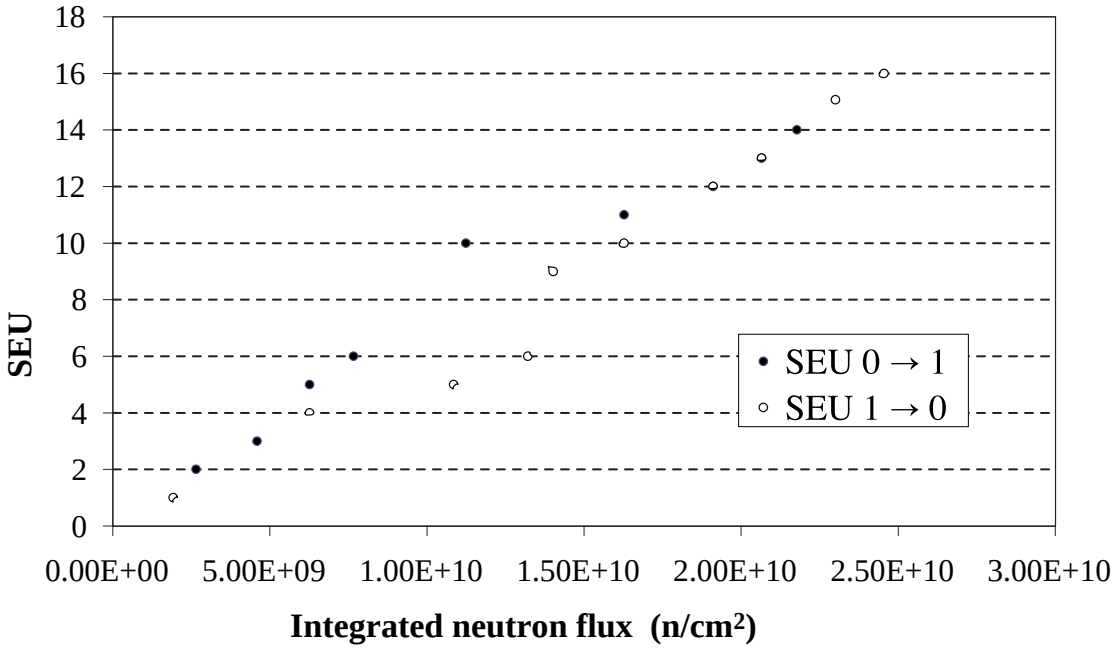


Figure 12 – SEU on SRAM#1 divided by type of bit modification

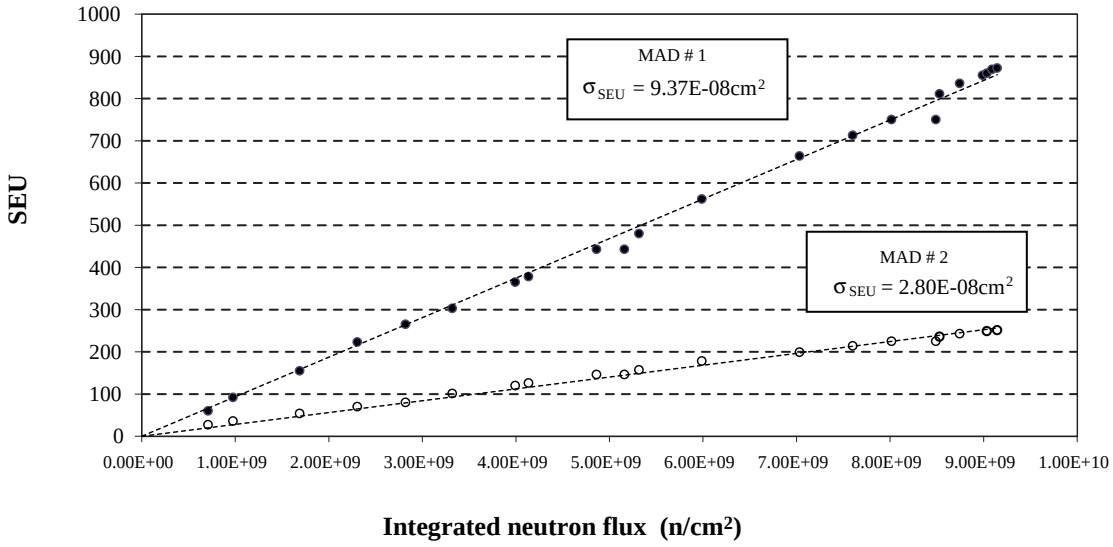


Figure 13- SEE on the front end device in thermal neutrons run.

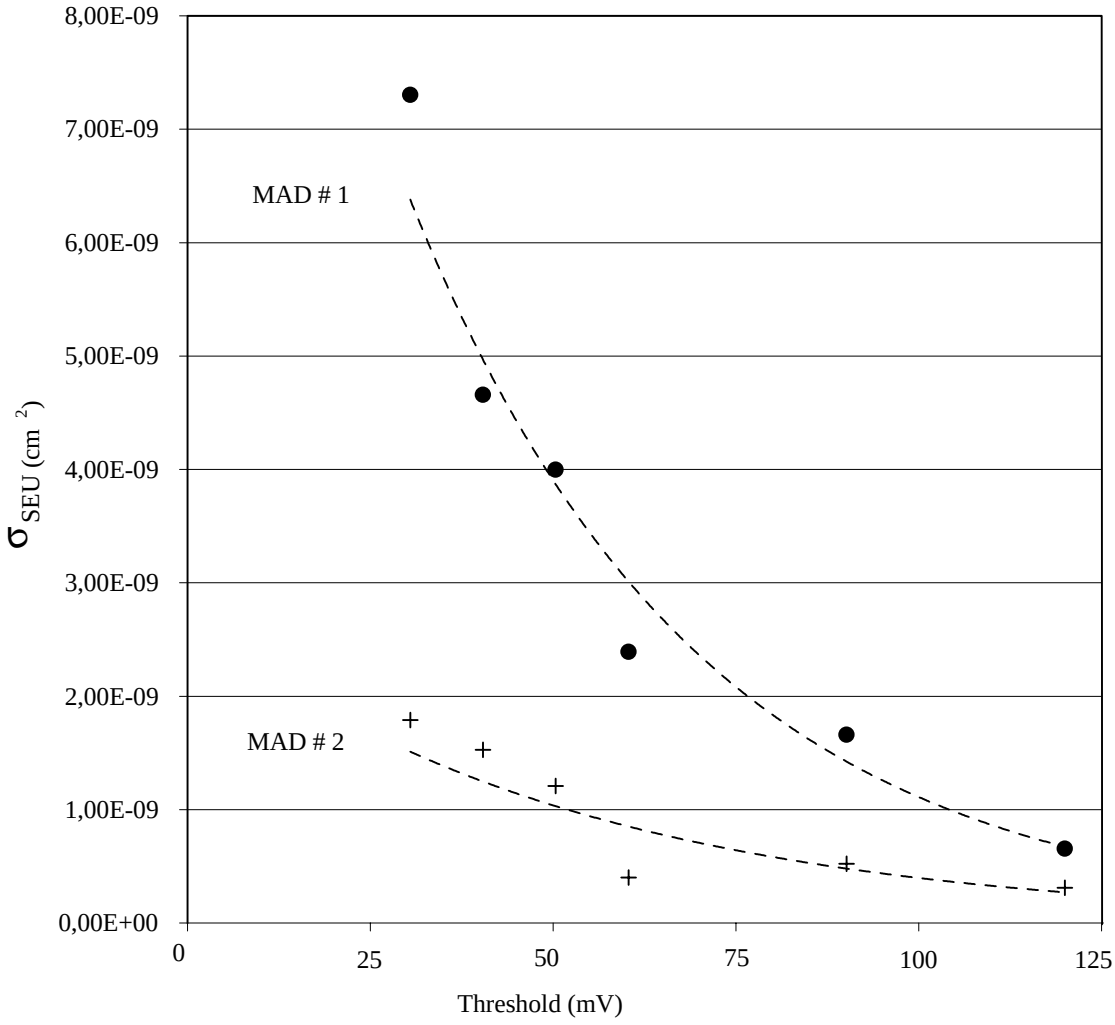


Figure 14 – SEE on front-end device as a function of discriminator threshold in fast neutrons run.

## 8. Radiation damage verification

After the whole bunch of tests, each device had received a dose greater than $10^{12}$ n/cm$^2$, equivalent to the expected dose after more than ten years of operation at LHC. We therefore verified the status of each device after irradiation, in order to see if the neutrons had produced any permanent damage. The only device showing a measurable deterioration was the Trigger Server ASIC (TSS), which was drawing a standby current increased by 10% with respect to the same current as measured before the tests. Besides none of the devices underwent a destructive SEE, but the test neutron energy could be too low to release enough charge.

## 9. Conclusions

We found evidence of neutrons induced SEE both in the fast energy region up to 11 MeV and in the thermal energy region.

We could give a first measurement of SEU cross section or derive upper limits for some devices to be used in the muon barrel electronics.

Efforts are being made in order to find energy or threshold dependence of the cross section using monochromatic neutron sources.

Besides higher neutron energies are needed to complete the exploration of the expected neutron energy range in CMS.

We believe that given the complexity of the observed phenomenology it is not possible to establish a safe test procedure to validate single components before ending these investigations.


## Acknowledgements

We thank the INFN Legnaro National Laboratory for providing us the help needed in the measurement setup. In particular we acknowledge the support received for the test by Dr. P. Colautti, CN accelerator coordinator, and the stimulating discussions we had with Dr. R. Cherubini.


## *References*


[1] CMS Muon Technical Proposal, CERN/LHCC 97-32, 1997.
[2] P.E. Dodd et al., IEEE Trans. On Nucl. Science, vol.43, No.6, Dec 1996.
[3] R. Katz et al., IEEE Trans. On Nucl. Science, vol.41, No.6, Dec 1994
K. A. LaBel et al., IEEE Trans. On Nucl. Science, vol.43, No.2, Apr 1996
[4] D.L. Oberg et al., IEEE Trans. On Nucl. Science, vol.43, No.6, Dec 1996
[5] P.J. Griffin et al., IEEE Trans. On Nucl. Science, vol.44, No.6, Dec 1997
[6] E. Normand, IEEE Trans. On Nucl. Science, vol.45, No.6, Dec 1998
[7] C. Vial et al., IEEE Trans. On Nucl. Science, vol.45, No.6, Dec 1998
[8] K. Johansson et al., IEEE Trans. On Nucl. Science, vol.45, No.6, Dec 1998
[9] E. Normand et al., IEEE Trans. On Nucl. Science, vol.41, No.6, Dec 1994
[10] K. Johansson et al., IEEE Trans. On Nucl. Science, vol.45, No.3, Jun 1998
[11] S. Duzellier et al., IEEE Trans. On Nucl. Science, vol.44, No.6, Dec 1997
[12] J. W. Meadows, Nucl. Instr. and Meth. A324 (1993) 239.
D.L. Smith et al.,Nucl. Instr. and Meth. A241 (1985) 507.
[13] S. Agosteo et al., Advances in Neutron Capture Therapy, Vol 1, 1997
S. Agosteo et al, Radiation Protection Dosimetry, Vol. 70, p. 559 (1997)